Geophysical Journal International

Geophys. J. Int. (2018) **213,** 426–433
Advance Access publication 2018 January 9
GJI Seismology

doi: 10.1093/gji/ggy003

A new fifth parameter for transverse isotropy III: reflection and transmission coefficients

Hitoshi Kawakatsu

Earthquake Research Institute, The University of Tokyo, Tokyo 113-0032*, Japan. E-mail:* hitosi@eri.u-tokyo.ac.jp

Accepted 2017 December 21. Received 2017 December 4; in original form 2017 August 4

SUMMARY

The effect of the newly defined fifth parameter, η_κ, of transverse anisotropy to the reflection and transmission coefficients, especially for *P*-to-*S* and *S*-to-*P* conversion coefficients, is examined. While η_κ systematically affects the *P*-to-*S* and *S*-to-*P* conversions, in the incidence angle range of the practical interest of receiver function studies, the effect may be asymmetric in a sense that *P*-wave receiver function is affected more than *S*-receiver function in terms of amplitude. This asymmetry may help resolving η_κ via extensive receiver function analysis. It is also found that *P*-wave anisotropy significantly influences *P*-to-*S* and *S*-to-*P* conversion coefficients that complicates the interpretation of receiver functions, because, for isotropic media, we typically attribute the primary receiver function signals to *S*-wave velocity changes but not to *P*-wave changes.

Key words: Composition and structure of the mantle; Body waves; Crustal imaging; Seismic anisotropy; Seismic anisotropy; Wave propagation; Wave scattering and diffraction.

INTRODUCTION

In a series of papers, Kawakatsu *et al.* (2015), Kawakatsu (2016a) and Kawakatsu (2016b) introduced a new parameter, η_κ,

$$\eta_\kappa = \frac{F+L}{(A-L)^{1/2}(C-L)^{1/2}}, \quad (1)$$

where A, C, F and L denote Love's elastic constants for transverse isotropy (TI; Love 1927), that characterizes the incidence angle dependence (relative to the symmetry axis) of seismic body wave velocities in a TI system. While the commonly used fifth parameter in global seismology, $\eta = F/(A-2L)$ (e.g. Anderson 1961; Takeuchi & Saito 1972), has no physical meaning, the newly defined parameter measures the departure from the 'elliptic condition' (Thomsen 1986) when η_κ is not equal to unity, and characterizes the incidence angle dependence of body waves (Kawakatsu 2016a). Kawakatsu (2016b) further demonstrated that, with the properly defined new set of parameters, sensitivities of those parameters to surface phase velocity or normal mode eigenfrequency made more sense, and thus they were useful for long-period seismology, as well as for body wave seismology and should be used to characterize vertical transverse isotropy (VTI) systems, particularly the lithosphere-asthenosphere system (LAS) where the presence of strong anisotropy had been well recognized (e.g. Forsyth 1975; Dziewonski & Anderson 1981).

Considering that η_κ describes the incidence angle dependence of body waves, it should also properly characterize the reflection/conversion characteristics between two VTI media. While the reflection property of *P*-wave in VTI media is extensively studied in exploration seismology (e.g. Rüger 1997; Tsvankin 2001), conversions of *P*-to-*S* and *S*-to-*P* that are essential for the receiver function (RF) study in global (or earthquake) seismology might have not been received enough attention. This short note attempts to cover that aspect, hoping it will be useful to characterize the LAS or seismic discontinuities therein. One of the interesting surprises is that *P*-wave anisotropy strongly influences the conversion efficiency of *P*-to-*S* and *S*-to-*P*, and thus may be resolved by using RFs. Also the effect of η_κ on conversion efficiency of *P*-to-*S* and *S*-to-*P* is different that may help resolving this parameter from the difference of amplitude of *P*-RFs and S-RFs.

REPRESENTATION OF RADIAL ANISOTROPY OR VTI

In a VTI system, horizontally and vertically propagating *P*-waves have phase velocities of

$$\alpha_H = \sqrt{A/\rho} \quad (2)$$

and

$$\alpha_V = \sqrt{C/\rho}, \tag{3}$$

respectively, where ρ gives the density. As to shear waves, the situation is slightly more complicated: while horizontally and vertically polarized *horizontally propagating S-waves* respectively have phase velocities of

$$\beta_H = \sqrt{N/\rho} \tag{4}$$

and

$$\beta_V = \sqrt{L/\rho}, \tag{5}$$

vertically propagating S-waves also have a phase velocity of β_V (*cf.* fig. 1 of Kawakatsu (2016a)). So for these horizontally or vertically travelling body waves, phase velocities are given by the four elastic constants, A, C, L and N, and the ratios of these elastic constants define the degree of anisotropy,

$$\varphi = C/A = \alpha_V^2/\alpha_H^2 \tag{6}$$

for P-wave, and

$$\xi = N/L = \beta_H^2/\beta_V^2 \tag{7}$$

for S-wave (Takeuchi & Saito 1972). For other intermediate direction body waves, the fifth elastic constant, F, affects the incidence angle dependence of quasi-P and quasi-SV waves via η_κ (Kawakatsu 2016a). It is also common, in global seismology, to use (α_H, β_V, ξ, ϕ, $\eta_\kappa(\eta)$), or (α_H, α_V, β_V, β_H, η_κ), as parameters instead of the original Love's elastic constants (Kawakatsu 2016b).

The VTI system is also extensively investigated in exploration seismology where the Thomsen parameters (Thomsen 1986) are commonly used for 'weak anisotropy':

$$\varepsilon = \frac{A-C}{2C} = \frac{1}{2}(\varphi^{-1} - 1) \tag{8}$$

$$\gamma = \frac{N-L}{2L} = \frac{1}{2}(\xi - 1) \tag{9}$$

$$\delta = \frac{(F+L)^2 - (C-L)^2}{2C(C-L)}. \tag{10}$$

While ε and γ are directly related to φ and ξ as shown above and thus to P- and S-wave anisotropy, δ was introduced such that it dominates in v_P in the case of near vertical incidence as in reflection profiling. In exploration seismology, it is common to use (α_V, β_V, ε, γ, δ) to represent VTI (Thomsen 1986). In addition, another parameter σ is introduced to make various expressions more tractable for weak anisotropy (Tsvankin & Thomsen 1994; Tsvankin 1995; Rüger 2001) that is related to η_κ as,

$$\sigma = \frac{\alpha_V^2}{\beta_V^2}(\varepsilon - \delta) \tag{11}$$

$$= \frac{1}{2}\left(1 - \eta_\kappa^2\right)\left(\frac{A}{L} - 1\right) \tag{12}$$

~1/2 (

(Kawakatsu *et al.* 2015).

REFLECTION AND TRANSMISSION COEFFICIENTS

The reflection and transmission coefficients for VTI media have been studied by many authors (e.g. Daley & Hron 1977; Graebner 1992). Here, we consider structures that mimic the lithosphere–asthenosphere system in the oceanic environment; as for a reference isotropic case, the upper layer is given by a Poisson solid whose P-wave and S-wave velocities and density are given by $\alpha_1 = 8.0\,\mathrm{km\,s^{-1}}$, $\beta_1 = 4.6188\,\mathrm{km\,s^{-1}}$, and $\rho_1 = 3.3\,\mathrm{g\,cc^{-1}}$, and the lower layer with 5 per cent velocity reductions for both P and S, but without a density reduction. Fig. 1 shows transmission coefficients, $\acute{P}\acute{S}$, $\acute{S}\acute{P}$, and reflection coefficients, $\acute{P}\grave{P}$, $\acute{S}\grave{S}$ for various anisotropic cases as a function of incidence angle; we employ the notation of Aki & Richards (1980) where acute (e.g. $\acute{P}$) and grave (e.g. $\grave{S}$) accents indicate upgoing and downgoing plane waves, respectively; that is, $\acute{P}\acute{S}$ indicates a P-to-S transmission (conversion) coefficient at an interface for a plane wave incident from below [*cf.* Aki & Richards (1980) for further details]. For the sake of simplicity, we introduce anisotropy only for the lower layer. We employ the strength of P-wave (a_p) and S-wave (a_s) anisotropy to specify corresponding anisotropic velocities as

$$\alpha_{H,V} = \alpha_0(1 \mp a_p/2),$$

$$\beta_{H,V} = \beta_0(1 \mp a_s/2),$$

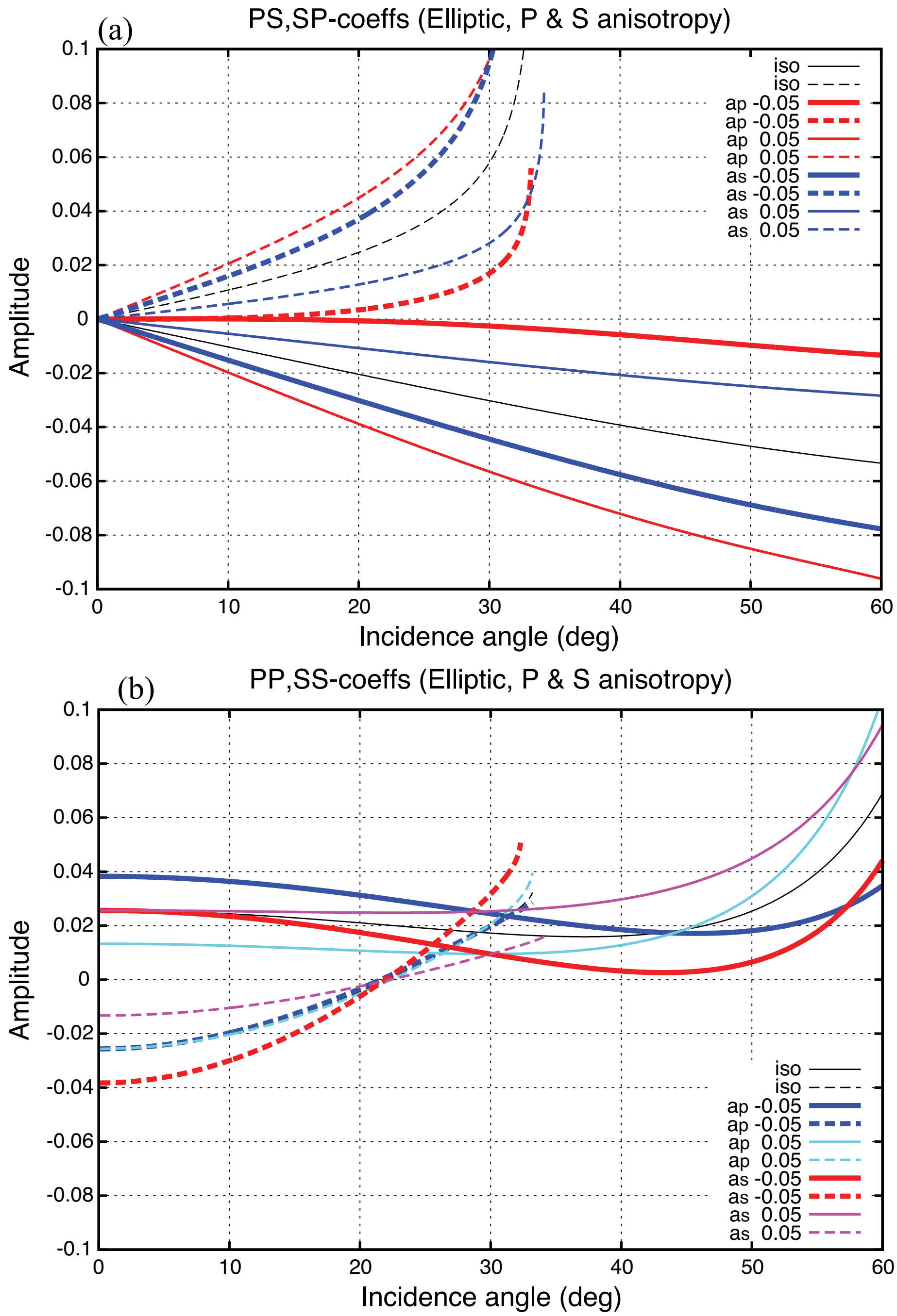

Figure 1. Effect of *P*-wave and *S*-wave anisotropy: (a) transmission coefficients $\acute{P}\acute{S}$ (solid lines) and $\acute{S}\acute{P}$ (broken lines), and (b) reflection coefficients $\acute{P}\grave{P}$ (solid lines) and $\acute{S}\grave{S}$ (broken lines). Those for the reference isotropic model are presented by grey colour.

where α_0 and β_0 denote the reference isotropic *P*-wave and *S*-wave velocities. In a VTI medium, as mentioned above, the phase velocity of either *P*- or *S*-wave is given as a function of incidence angle, and the ray parameter that is conserved across the interface is estimated from the phase velocity and the incidence angle in the conventional way of seismology.

In Fig. 1, we consider cases with a_p or a_s equals to ± 5 per cent. As *S*-wave anisotropy itself does not enter in the *P*/*SV* coupling in VTI, the effect of changing a_s is equivalent to that of isotropic *S*-wave; for example, $a_s = 5$ per cent makes β_V faster by 2.5 per cent, making the *S*-wave velocity reduction at the boundary smaller that results in smaller $\acute{P}\acute{S}$ and $\acute{S}\acute{P}$ (Fig. 1a). What is interesting here is that the introduction of *P*-wave anisotropy, $a_p = \pm 5$ per cent, causes large change in the conversion efficiency (larger than *S*-wave case). This is rather unexpected because, for the isotropic case, the effect of *P*-wave velocity (and density) change at the boundary has negligible effect on $\acute{P}\acute{S}$ and $\acute{S}\acute{P}$ (e.g. Aki & Richards 1980). As for reflection coefficients, the effect of *P*-wave anisotropy is quite small for $\acute{S}\grave{S}$ as expected, but that of *S*-wave for $\acute{P}\grave{P}$ becomes large as the incidence angle.

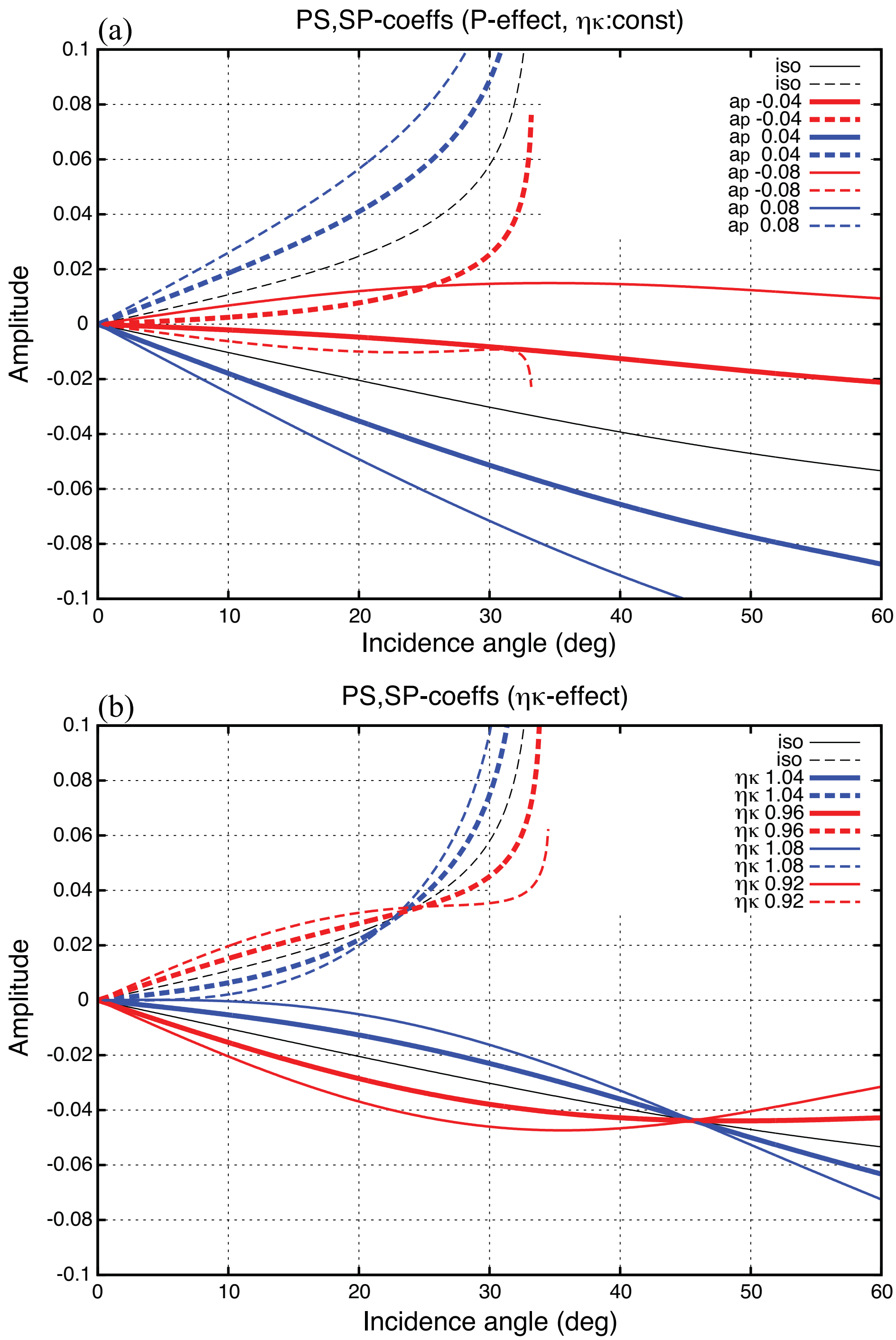

Figure 2. Effect of P-wave anisotropy (a) and η_κ (b) on $\acute{P}\acute{S}$ (solid lines) and $\acute{S}\acute{P}$ (broken lines). Other parameters are kept for the values of the reference isotropic model (grey).

Fig. 2(a) further examines the effect of P-wave anisotropy on the conversion efficiency. The effect is quite systematic and severe, and in the case when P-wave anisotropy exceeds ∼6 per cent both $\acute{P}\acute{S}$ and $\acute{S}\acute{P}$ appear to reverse the amplitude for this particular example. Considering that an increase of S-wave velocity in the lower layer by 5 per cent ($a_s = 10$ per cent in this parametrization) makes no discontinuity, we may be able to say that a similar effect can be obtained by setting $a_p = 6$ per cent. In terms of the shape of the curves, both effects are similar in a sense that the general characteristics do not change much. On the other hand, the effect of η_κ on the curve shape is quite different (Fig. 2b). This is expected as η_κ controls the incidence angle dependence of P- and S-wave phase velocities by introducing an additional convex or concave pattern when $\eta_\kappa \neq 1$. What should be noted here is that because of the above nature, there exist ranges of incidence angles that give stationary values for $\acute{P}\acute{S}$ and $\acute{S}\acute{P}$; for $\acute{P}\acute{S}$, this occurs around an incidence angle of 45°, much larger than the typical ones for P-RFs. On the other hand, the range for $\acute{S}\grave{P}$ is ∼22.5°–25°, a range that occurs for teleseismic *S*-RFs. This may introduce asymmetric effect of η_κ on *P*-RF and *S*-RF: while the amplitude of the *S*-to-*P* conversion phase in *S*-RF is not affected much by η_κ, that of *P*-to-*S* in *P*-RF might be.

DISCUSSION

Rüger (1997) derived an approximation formula for the *P* reflection coefficient between two VIT media with weak anisotropy and small parameter jumps, and Rüger (2001) published those for all other reflection or transmission coefficients. For $\grave{P}\acute{S}$ and $\acute{S}\grave{P}$, his formula may be reorganized as,

$$\grave{P}\acute{S} = \left[\frac{\sin i}{\cos j}\right] \cdot \left[\left(\frac{1}{2} - R\cos i\cos j - R^2\sin^2 i\right) \cdot \left(\frac{\Delta\rho}{\rho}\right) - 2\left(R\cos i\cos j + R^2\sin^2 i\right) \cdot \left(\frac{\Delta\beta_V}{\beta_V}\right) - \frac{1}{1-R^2}\left(1 + R\cos i\cos j - R^2\sin^2 i\right) \cdot \left(\frac{1}{2}\Delta\delta - (\Delta\delta - \Delta\epsilon)\sin^2 i\right)\right] \tag{13}$$

$$\acute{S}\grave{P} = -\left[\frac{\sin j}{\cos i}\right] \cdot \left[\left(\frac{1}{2} - R\cos i\cos j - \sin^2 j\right) \cdot \left(\frac{\Delta\rho}{\rho}\right) - 2\left(R\cos i\cos j + \sin^2 j\right) \cdot \left(\frac{\Delta\beta_V}{\beta_V}\right) - \frac{1}{1-R^2}\left(1 + R\cos i\cos j - \sin^2 j\right) \cdot \left(\frac{1}{2}\Delta\delta - (\Delta\delta - \Delta\epsilon)R^{-2}\sin^2 j\right)\right], \tag{14}$$

where i and j respectively refer to the incidence angles (measured from the vertical symmetry axis) of *P*- and *S*-wave in the lower layer, $R = \beta_V/\alpha_V$ and $\Delta\chi = \chi_{\rm upper} - \chi_{\rm lower}$ for $\chi = \{\rho, \beta_V, \delta, \epsilon\}$. α_V, β_V and ρ are the average values of two layers. The first two terms of each coefficient are equivalent to those given by Aki & Richards (1980) for an isotropic medium.

By noting that $R\sin i \approx \sin j$ (Snell's law for isotropic case) to the zeroth order in small perturbations, the above equations may be written as,

$$\grave{P}\acute{S} = \frac{1}{2}\left[\frac{\sin i}{\cos j}\right] \cdot \left[\left(1 - 2R\cos i\cos j - 2R^2\sin^2 i\right) \cdot \left(\frac{\Delta\rho}{\rho}\right) - 4\left(R\cos i\cos j + R^2\sin^2 i\right) \cdot \left(\frac{\Delta\beta_V}{\beta_V}\right) - \frac{1 + R\cos i\cos j - R^2\sin^2 i}{1-R^2} \cdot \left(\Delta\epsilon - R^2\cos 2i\,\Delta\sigma\right)\right] \tag{15}$$

$$\acute{S}\grave{P} = -\left[\frac{\sin j}{\cos i} \cdot \frac{\cos j}{\sin i}\right]\grave{P}\acute{S}. \tag{16}$$

Fig. 3(a) evaluates the approximate expressions in comparison with the exact solutions. The comparison indicates Rüger (2001)'s approximations are useful except near the critical angle for $\acute{S}\grave{P}$; although the approximation is not so useful near the critical angle, if the ratio of the transmitted energy over the incident energy is low, it may not be a severe problem. In Fig. 3(b), Rüger's expressions are used to evaluate the sensitivity of the different parameters to the conversion coefficients (i.e. terms related to $\Delta\rho/\rho$, $\Delta\beta_V/\beta_V$, $\Delta\epsilon$, $\Delta\sigma$) as given in eqs. (15) and (16). The well-known fact for the isotropic case that *PS* and *SP* conversions have a strong sensitivity to *S*-wave velocity (red lines) but weak one to density (black lines) can be observed. For the case of VTI, both $\Delta\epsilon$ and $\Delta\sigma$ show sensitivity. The strong sensitivity of $\Delta\epsilon$ (*P*-wave anisotropy) is rather unexpected as *P*-wave velocity jump, $\Delta\alpha_V/\alpha_V$, has no major effect on PS and SP conversions for isotropic case as the corresponding term being absent in eqs. (15) and (16). This effect might severely bias the interpretation of receiver functions. For example, Fig. 3(b) indicates that the effect of $\Delta\epsilon$ (blue lines) is very similar to that of $\Delta\beta_V/\beta_V$ (red lines). It should be also noted that this strong effect of *P*-anisotropy is not due to a change in *F* while keeping η_κ constant. A change solely made for *A* and *C* also shows a similar strong effect. For waves incident from above, the same effect (but the opposite sign) of *P*-wave anisotropy is expected as evident from a comparison of $\grave{P}\acute{S}$ (15), $\acute{S}\grave{P}$ (16) and $\acute{P}\grave{S}$ (A6), $\grave{S}\acute{P}$ (A8) in the Appendix. Fig. 3(b) also indicates strong sensitivities for $\Delta\rho/\rho$ and $\Delta\sigma$ near the critical angle for $\acute{S}\grave{P}$, but this should not be exploited because the transmitted energy is very low near critical angle, besides the inaccuracy of the approximation itself therein.

Kawakatsu (2016b) has shown that, with the properly defined set of VTI parameters using η_κ, the previously claimed sensitivity of spheroidal mode eigenfrequencies to *P*-wave anisotropy is largely due to the effect of β_V improperly mapped into the *P*-wave anisotropy sensitivity kernel, and actual sensitivity kernels are much more reduced in amplitude [e.g. fig. 2 of Kawakatsu (2016b)]. Careful examination of the figure, however, indicates that *P*-wave anisotropy has substantial increased sensitivity for the shallow part, especially near the surface. This may be in part due to the *P*-to-*S* or *S*-to-*P* conversion effect in the anisotropic shallow ∼200 km layers in PREM (Dziewonski & Anderson 1981), as well as due to the *P*-to-*S* and *S*-to-*P* conversions in the surface reflections. The sharpened strong sensitivity of *P*-wave anisotropy at the surface may deserve further attention in the interpretation of ambient noise Rayleigh wave dispersion measurements (e.g. Shapiro *et al.* 2005; Lin *et al.* 2010).

The strong influence of *P*-wave anisotropy to *P*-to-*S* and *S*-to-*P* conversion coefficients revealed in the this study may deserve attention in regard to the receiver function analysis because, for isotropic media, we typically attribute the primary receiver function signals to *S*-wave velocity changes, but not to *P*-wave changes. Considering that the receiver function analysis has become a popular and powerful tool to

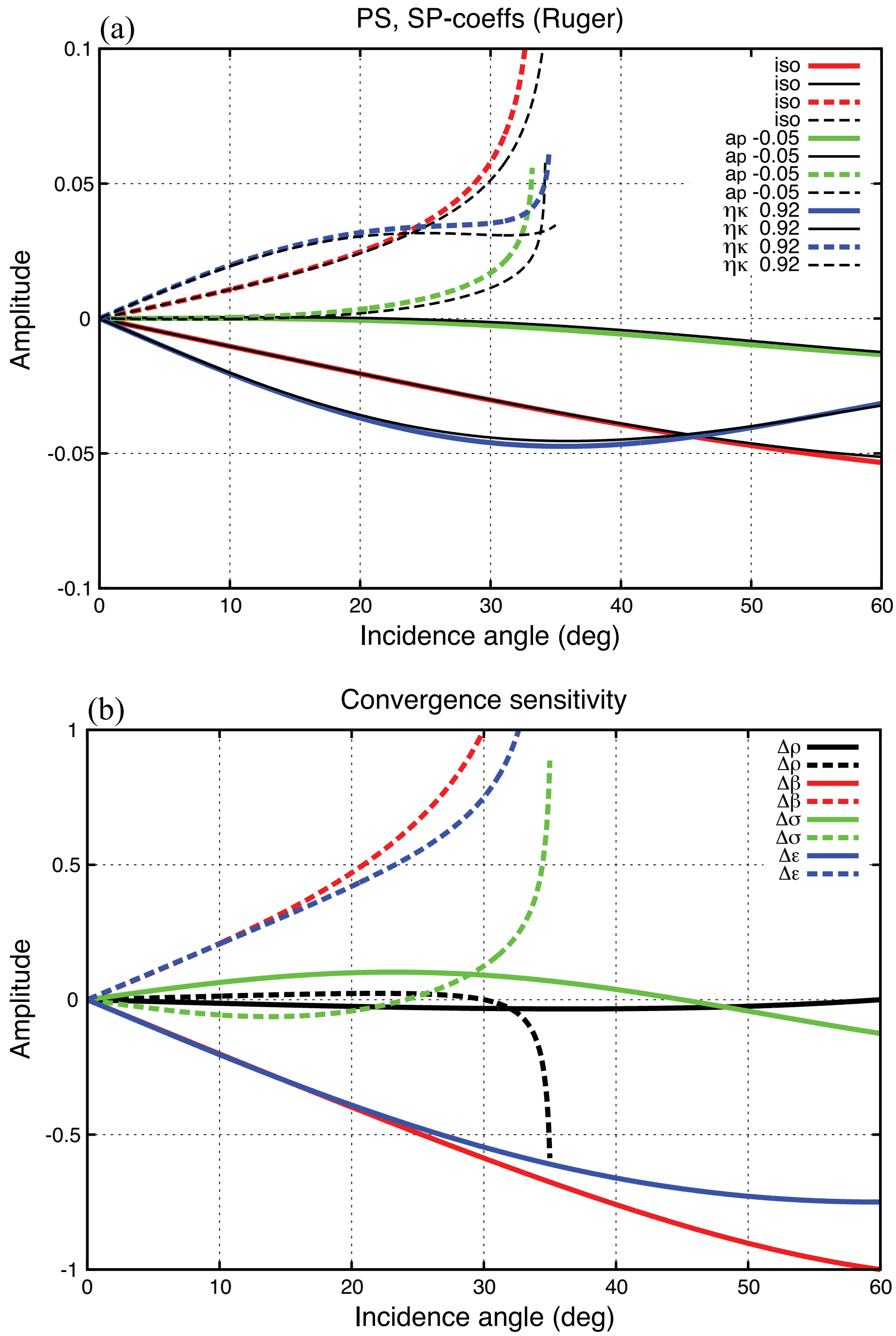

Figure 3. (a) Comparison of exact solutions (grey) and Ruger's approximations (coloured) of $\acute{P}\acute{S}$ (solid lines) and $\acute{S}\acute{P}$ (broken lines) for various anisotropy. (b) Sensitivities of anisotropic parameters to $\acute{P}\acute{S}$ (solid lines) and $\acute{S}\acute{P}$ (broken lines). Note that the sensitivity of $\Delta\epsilon$ (blue) is large and comparable to that of $\Delta\beta/\beta$ (red).

investigate the crustal and upper mantle structures, such as Moho (e.g. Bodin *et al.* 2014), the mid-lithospheric discontinuity (e.g. Abt *et al.* 2010) and the G-discontinuity (sometime referred to just as lithosphere-asthenosphere boundary) (e.g. Rychert *et al.* 2005; Kawakatsu *et al.* 2009; Kumar *et al.* 2012), it seems important to fully understand to what extent and under what circumstances the effect might be significant.

ACKNOWLEDGEMENTS

This research is partly supported by JSPS KAKENHI 15K13558, 15H05832 and 17H02948.

REFERENCES

Abt, D.L., Fischer, K.M., French, S.W., Ford, H.A., Yuan, H. & Romanowicz, B., 2010. North American lithospheric discontinuity structure imaged by Ps and Sp receiver functions, *J. geophys. Res.,* **115,** B09301. doi:10.1029/2009JB006914.

Aki, K. & Richards, P., 1980. *Quantitative Seismology: Theory and Methods,* W. H. Freeman.

Anderson, D.L., 1961. Elastic wave propagation in layered anisotropic media, *J. geophys. Res.,* **9,** 2953–2963.

Bodin, T., Yuan, H. & Romanowicz, B., 2014. Inversion of receiver functions without deconvolution—application to the Indian Craton, *Geophys. J. Int.,* **196,** 1025–1033.

Daley, P.F. & Hron, F., 1977. Reflection and transmission coefficients for transversely isotropic media, *Bull. seism. Soc. Am.,* **67,** 661–675.

Dziewonski, A.M. & Anderson, D.L., 1981. Preliminary reference Earth model, *Phys. Earth planet. Inter.* **25,** 297–356.

Forsyth, D.W., 1975. The early structural evolution and anisotropy of the oceanic upper mantle, *Geophys. J. R. astr. Soc.* **43,** 103–162.

Graebner, M., 1992. Plane-wave reflection and transmission coefficients for a transversely isotropic solid, *Geophysics,* **57,** 1512–1519.

Kawakatsu, H., 2016a. A new fifth parameter for transverse isotropy, *Geophys. J. Int.,* **204,** 682–685.

Kawakatsu, H., 2016b. A new fifth parameter for transverse isotropy II: partial derivatives, *Geophys. J. Int.,* **206,** 360–367.

Kawakatsu, H., Kumar, P., Takei, Y., Shinohara, M., Kanazawa, T., Araki, E. & Suyehiro, K., 2009. Seismic evidence for sharp lithosphere-asthenosphere boundaries of oceanic plates, *Science,* **324,** 499–502.

Kawakatsu, H., Montagner, J.P. & Song, T.R.A., 2015. On DLA's η, in *The Interdisciplinary Earth: A Volume in Honor of Don L. Anderson,* pp. 33–38, GSA and AGU.

Kumar, P., Kind, R., Yuan, X. & Mechie, J., 2012. USArray receiver function images of the lithosphere-asthenosphere boundary, *Seismol. Res. Lett.,* **83,** 486–491.

Lin, F.C., Ritzwoller, M.H., Yang, Y., Moschetti, M.P. & Fouch, M.J., 2010. Complex and variable crustal and uppermost mantle seismic anisotropy in the western United States, *Nat. Geosci.,* **4,** 55–61.

Love, A.E.H., 1927. *A Treatise on the Mathematical Theory of Elasticity,* Dover.

Rüger, A., 1997. *P*-wave reflection coefficients for transversely isotropic models with vertical and horizontal axis of symmetry, *Geophysics,* **62,** 713–722.

Rüger, A., 2001. *Reflection Coefficients and Azimuthal AVO Analysis in Anisotropic Media,* Society of Exploration Geophysics, 189 pp.

Rychert, C.A., Fischer, K.M. & Rondenay, S., 2005. A sharp lithosphere-asthenosphere boundary imaged beneath eastern North America, *Nature,* **436,** 542–545.

Shapiro, N.M., Campillo, M., Stehly, L. & Ritzwoller, M.H., 2005. High-resolution surface-wave tomography from ambient seismic noise, *Science,* **307,** 1615–1618.

Takeuchi, H. & Saito, M., 1972. Seismic surface waves, in *Seismology: Surface Waves and Earth Oscillations, Methods in Computational Physics,* Vol. 11, pp. 217–295, Academic Press.

Thomsen, L., 1986. Weak elastic anisotropy, *Geophysics,* **51,** 1954–1966.

Tsvankin, I., 1995. Body-wave radiation patterns and AVO in transversely isotropic media, *Geophysics,* **60,** 1409–1425.

Tsvankin, I., 2001. *Seismic Signatures and Analysis of Reflection Data in Anisotropic Media,* Pergamon Press, 436 pp.

Tsvankin, I. & Thomsen, L., 1994. Nonhyperbolic reflection moveout in anisotropic media, *Geophysics,* **59,** 1290–1304.

APPENDIX: RUGER'S APPROXIMATION REFLECTION AND TRANSMISSION COEFFICIENTS

Here we reproduce Rüger (2001) equations in a form discussed in this manuscript. The reflection and transmission coefficients are given using the notation of Aki & Richards (1980), and only cases with *P*-wave and *S*-wave incident from the upper layer are considered (opposite to the case in the main text where upgoing incidence cases are considered). i and j respectively refer to the incidence angles (measured from the vertical symmetry axis) of *P*- and *S*-wave in the upper layer, and $R = \beta_V/\alpha_V$ and $\Delta\chi = \chi_{\text{lower}} - \chi_{\text{upper}}$ for $\chi = \{\rho, \alpha_V, \beta_V, \delta, \epsilon, \gamma\}$. α_V, β_V, and ρ are the average values of two layers. The terms with $\Delta\alpha_V$, $\Delta\beta_V$, $\Delta\rho$ of each coefficient are equivalent to those given by Aki & Richards (1980) for an isotropic medium. $R\sin i \approx \sin j$ (Snell's law for isotropic case) is sometimes employed to simplify the expression. It is worth mentioning that $\grave{P}\grave{S}$ and $\grave{S}\grave{P}$ keep the same scaling as for the case of isotropy (Aki & Richards 1980), while $\grave{P}\acute{S}$ and $\grave{S}\acute{P}$ do not.

P–SV:

$$\grave{P}\acute{P} = \frac{1}{2}\left(1 - 4R^2\sin^2 i\right)\cdot\left(\frac{\Delta\rho}{\rho}\right) + \frac{1}{2\cos^2 i}\left(\frac{\Delta\alpha_V}{\alpha_V}\right) - 4R^2\sin^2 i\left(\frac{\Delta\beta_V}{\beta_V}\right) + \frac{1}{2}\sin^2 i\left(\frac{1}{\cos^2 i}\Delta\epsilon - R^2\Delta\sigma\right) \tag{A1}$$

$$\grave{P}\grave{P} = 1 - \frac{1}{2}\left(\frac{\Delta\rho}{\rho}\right) + \left(\frac{1}{2\cos^2 i} - 1\right)\left(\frac{\Delta\alpha_V}{\alpha_V}\right) + \frac{1}{2}\sin^2 i\left(\frac{1}{\cos^2 i}\Delta\epsilon - R^2\cos 2i\,\Delta\sigma\right) \tag{A2}$$

$$\grave{S}\acute{S} = -\frac{1}{2}\left(1 - 4\sin^2 j\right)\cdot\left(\frac{\Delta\rho}{\rho}\right) - \left(\frac{1}{2\cos^2 j} - 4\sin^2 j\right)\left(\frac{\Delta\beta_V}{\beta_V}\right) + \frac{1}{2}\sin^2 j\,\Delta\sigma \tag{A3}$$

$$\grave{S}\grave{S} = 1 - \frac{1}{2}\left(\frac{\Delta\rho}{\rho}\right) + \left(\frac{1}{2\cos^2 j} - 1\right)\left(\frac{\Delta\beta_V}{\beta_V}\right) + \frac{1}{2}\sin^2 j\cos 2j\,\Delta\sigma \tag{A4}$$

$$\begin{aligned}\grave{P}\acute{S} = -\frac{1}{2}\left[\frac{\sin i}{\cos j}\right]\cdot\Bigg[&\left(1 + 2R\cos i\cos j - 2R^2\sin^2 i\right)\cdot\left(\frac{\Delta\rho}{\rho}\right) + 4\left(R\cos i\cos j - R^2\sin^2 i\right)\cdot\left(\frac{\Delta\beta_V}{\beta_V}\right)\\ &+\left(\frac{R\cos i\cos j - 1}{1 - R^2}\right)\left(\Delta\epsilon - R^2\cos 2i\,\Delta\sigma\right)\Bigg]\end{aligned} \tag{A5}$$

$$\grave{P}\grave{S} = \frac{1}{2}\left[\frac{\sin i}{\cos j}\right]\cdot\left[\left(1 - 2R\cos i\cos j - 2R^2\sin^2 i\right)\cdot\left(\frac{\Delta\rho}{\rho}\right) - 4\left(R\cos i\cos j + R^2\sin^2 i\right)\cdot\left(\frac{\Delta\beta_V}{\beta_V}\right)\right.$$
$$\left. - \left(\frac{1 + R\cos i\cos j - R^2\sin^2 i}{1 - R^2}\right)\left(\Delta\epsilon - R^2\cos 2i\,\Delta\sigma\right)\right] \tag{A6}$$

$$\grave{S}\acute{P} = -\frac{1}{2}\left[\frac{\sin j}{\cos i}\right]\cdot\left[\left(1 + 2R\cos i\cos j - 2\sin^2 j\right)\cdot\left(\frac{\Delta\rho}{\rho}\right) + 4\left(R\cos i\cos j - \sin^2 j\right)\cdot\left(\frac{\Delta\beta_V}{\beta_V}\right)\right.$$
$$\left. + \left(\frac{R\cos i\cos j - \cos^2 j}{1 - R^2}\right)\left(\Delta\epsilon - R^2\cos 2i\,\Delta\sigma\right)\right] \tag{A7}$$

$$\grave{S}\grave{P} = -\left[\frac{\sin j}{\cos i}\cdot\frac{\cos j}{\sin i}\right]\grave{P}\grave{S}. \tag{A8}$$

SH:

$$\grave{S}\acute{S} = -\frac{1}{2}\left(\frac{\Delta\rho}{\rho}\right) + \left(\frac{1}{2\cos^2 j} - 1\right)\left(\frac{\Delta\beta_V}{\beta_V}\right) + \frac{1}{2}\tan^2 j\,\Delta\gamma \tag{A9}$$

$$\grave{S}\grave{S} = 1 - \frac{1}{2}\left(\frac{\Delta\rho}{\rho}\right) + \left(\frac{1}{2\cos^2 j} - 1\right)\left(\frac{\Delta\beta_V}{\beta_V}\right) + \frac{1}{2}\tan^2 j\,\Delta\gamma. \tag{A10}$$